DOI: https://doi.org/10.54966/jreen.v27i2.1201

Journal of Renewable Energies

Revue des Energies Renouvelables

journal home page: https://revue.cder.dz/index.php/rer

Research paper

Analysis of a simple vapor compression and ejector refrigeration system working with eco-friendly refrigerants

Halla Aissani [a,*], **Said Zid** [a], **Mehdi Bencharif** [b]

[a] *LGCC, Faculty of frères Mentouri, university of Constantine 1, campus Ahmed Hamani 25017 Constantine, Algeria*

[b] *Mechanical Engineering Department, University of Sherbrooke, Sherbrooke, Canada*

ARTICLE INFO

Article history:

Received May 15, 2024

Accepted December 1st, 2024

Keywords:

Thermodynamic model,
Vapor compression,
Ejector,
COP,
GWP.

ABSTRACT

Transitioning to alternative refrigerants with low Global Warming Potential (GWP) in both vapor compression and ejector refrigeration systems emerges as a viable strategy to address the environmental impact associated with refrigeration technologies. This shift necessitates a thorough examination of factors such as thermodynamic performance, safety considerations, and optimization of system design. The outcomes of this study contribute to the advancement of sustainable refrigeration systems, aligning with global initiatives to curb greenhouse gas emissions and preserve the environment.

The study adopts a thermodynamic approach to numerically investigate several eco-friendly refrigerants with GWP below 150, including R1234yf, R1234ze, R1270, R152a, R290, and R600a, as potential alternatives for vapor compression and ejector refrigeration systems. Thermodynamic models, developed in MATLAB using refrigerant properties, reveal that R600a and R290 exhibit promising potential as replacements for R134a in vapor compression refrigeration systems. These alternatives demonstrate a noteworthy improvement in the thermodynamic coefficient of performance, with percentages of 2.47% and 2.12%, respectively, under similar working conditions.

For ejector refrigeration systems, R152a, R717, and R1270 exhibit enhanced coefficients of performance, contributing to significant savings in generator heat load. The results highlight the ability of these refrigerants to improve both the efficiency and sustainability of refrigeration systems in diverse applications.

1. INTRODUCTION

The detrimental environmental impacts associated with conventional refrigerants, such as

* *Corresponding author, E-mail address: hala.aissani@doc.umc.edu.dz*

ISSN: 1112-2242 / EISSN: 2716-8247

hydrofluorocarbons (HFCs), have led to the urgent need for more sustainable alternatives and the choice of refrigerant fluids used in cooling and refrigeration systems plays a vital role in ensuring both the systems' efficient operation and environmental sustainability. With increasing concerns about climate change and the depletion of the ozone layer, the importance of using safe refrigerant fluids has become paramount. Protocols and new regulations (F-gas) of the European Union have dictated the HFC phase down and restriction of refrigerants with global warming potential (GWP) above 150 and phased out the use of R134a in automotive air conditioning systems for all new models in 2011 **(** Directive 2006/40/EC of the European Parliament**)**, and set a goal to cut emissions of HFCs by two-thirds by 2030, which is all a part of the goal to attain climate neutrality by 2050.

In anticipation of these regulations, extensive research has been carried out to select the best potential alternative refrigerants that could be used as a drop-in replacement for conventional refrigerants. However, it's evident that these substitutes, including natural refrigerants like R600a, R290, and R1270, present challenges such as flammability, toxicity, and high working pressure. Despite these challenges, natural refrigerants offer several advantages, including low GWP, zero ozone depletion potential (ODP), and high thermodynamic efficiency. Safety considerations, such as flammability and toxicity, must be addressed through proper system design and safety measures (Zyczkowski, et al., 2020).

Various studies have explored the use of alternative refrigerants. An extensive study of potential R134a substitutes was carried out since it's about to be prohibited by the F-Gas regulation (Sánchez, et al, 2017). The study analyzed the performance of R290, R600a, R152a, R1234yf, and R1234ze (E) refrigerants. When R134a was replaced with R1234ze (E) using the drop-in method, there were significant reductions in cooling capacity and energy consumption, decreasing by 24.9% and 17.8%, respectively. Consequently, the COP decreased by approximately 8.6%. Among the refrigerants tested, R1234ze (E) exhibited the greatest increase in COP. However, achieving a cooling capacity similar to that of R134a would require a compressor with a larger cylinder capacity. (Bansal, et al, 2015), made a study on a window air conditioner, the R410A refrigerant was replaced with R32, the R32/R125 mixture, and with R600a, R290, R1234yf, R1234ze, and R134a. As far as the capacity was concerned, the best results were obtained with the R32 refrigerant (a 4% COP increase). The worst results were achieved by HFO refrigerants, i.e., R1234yf and R1234ze (E). A compressor with a higher cylinder capacity is required to obtain the same cooling capacity as R410A. (Ansari, et al, 2013) utilized an exergy analysis to theoretically compare R1234yf and R1234ze with R134a. Their findings indicated that the performance parameters of R1234yf were slightly lower than those of R134a, while those of R1234ze were nearly identical. Thus, both refrigerants can serve as substitutes for R134a, though minor design modifications are recommended when using R1234ze. This study highlighted that R1234ze and R1234yf can be good alternatives to R134a. (Zheng, et al, 2022) conducted an experimental investigation into using R290 as a substitute for R134a in a vapor compression cold storage air conditioning system. The results demonstrated that with a standard refrigerant charge, the R290 system offered benefits such as a rapid cooling rate and high refrigerant efficiency. While the refrigeration performance coefficient was comparable to that of R134a, the system could be further optimized by replacing the compressor and incorporating a high-efficiency heat exchanger. (Ozsipahi, et al, 2022) put forward an experimental study of R290/R600a refrigerant mixture in a vapor compression refrigeration system. The highest COP was found at the compression ratio of 8.9 using the 60% and 70% of R290 mass fraction. (Sánchez, et al, 2022) Evaluated the energy impact of six different low-GWP alternatives to replace R134a, results demonstrated that the use of R290, R1270, R744, and R600a allows energy savings, as for R1234yf, it increases the energy usage to 4.1%. (Colombo et al0, 2020) conducted an experimental study on using R1234yf and R1234ze (E) as drop-in replacements for R134a in a water-to-water heat pump. The findings revealed that R1234yf is better suited for low- and medium-temperature heat pump applications, while R1234ze (E) is more appropriate for high-temperature heat pumps. (de Paula, et al.,

2020) Established a thermo-economic and environmental analysis of a small-capacity vapor compression refrigeration system using R290, R1234yf, and R600a. Their findings showed that the system with R290 outperformed the other refrigerants in terms of energy efficiency, exergy, environmental impact, and economic viability, making it the most suitable alternative to replace R134a.

(Atmaca et al., 2017) examined the performance of ejectors as expansion devices in a vapor compression refrigeration cycle using R1234yf and R1234ze (E) as working fluids and compared the results to R134a. The study found that the COP and entrainment ratio for R1234ze (E) and R134a were similar and slightly higher than those for R1234yf. (Galindo et al., 2020) performed a numerical analysis of a solar jet ejector refrigeration system utilizing environmentally friendly refrigerants R1234yf, R1234ze, and R600a. The results indicated that R1234yf achieved the highest overall system efficiency, with R600a and R1234ze showing slightly lower performance. The same result was obtained by (Tashtoush et al., 2019) who made a comparative thermodynamic of several eco-friendly refrigerants used in a solar ejector cooling system, and the results showed that R1234yf has the best COP, high entrainment ratio, and its thermophysical properties were similar to those of R134a.

This paper extends the studies found in the literature and a more comprehensive approach is followed, based on both the first and second laws of thermodynamics. A thermodynamic model is developed to analyze and compare the performance of both, the simple vapor compression refrigeration system equipped with an internal heat exchanger to guarantee better performance and the ejector refrigeration system using the same eco-friendly refrigerants. After validating the obtained results of our model against several experimental results published in the literature. Results are discussed to determine the most suitable refrigerant for each installation and to investigate further optimization methods for better performance and less energy consumption possible. Followed by concluding remarks and perspectives of future works.

The criteria of refrigerant selection are based on several requirements such as being non-toxic, nonflammable, and noncorrosive for the mechanical components of the system. They must have good thermodynamic properties leading to high values of the COP as well as high densities at moderate pressures for both the liquid and vapor phases. Furthermore, their ozone depletion potential (ODP) and global warming potential (GWP) must be low.

Table 1. Properties of R1234yf, R1234ze, R600a, R290 and R1270 refrigerants (Bell et al., 2014)

Properties	**Molar mass (g/mol)**	**Tcrit (◦C)**	**Pcrit (bar)**	**NBP (◦C)**	**GWP 100**
R134a	102.03	101.1	40.6	-26.1	1300
R1234yf	114	94.7	33.8	-29.5	<1
R1234ze(E)	114	109.4	36.4	-19.3	7
R600a	58.12	134.7	36.3	-11.8	4
R290	44.10	96.7	42.5	-42.1	3
R1270	42	91.1	46.7	-47.6	2
R152a	66.05	113.15	44.96	-24.7	124

2. THERMODYNAMIC MODEL

A thermodynamic analysis was carried out using a computational model for a single-stage vapor compression cycle (Figure 1) and an ejector refrigeration system (Figure 2). The model was developed in MATLAB, utilizing COOLPROP to extract thermodynamic properties of refrigerants. COOLPROP

is a refrigerant library based on the Helmholtz free energy formulation, offering thermodynamic and transport data for various refrigerants over a specific range of parameters. A detailed literature review of experimental data on thermophysical properties of low-GWP refrigerants that are necessary to formulate accurate equations of state, and they are presented in details by (Bobbo et al., 2018).

2.1 The simple vapor compression system

Figure (1) shows a schematic representation of the system under consideration and the pressure-enthalpy diagram of the corresponding processes.

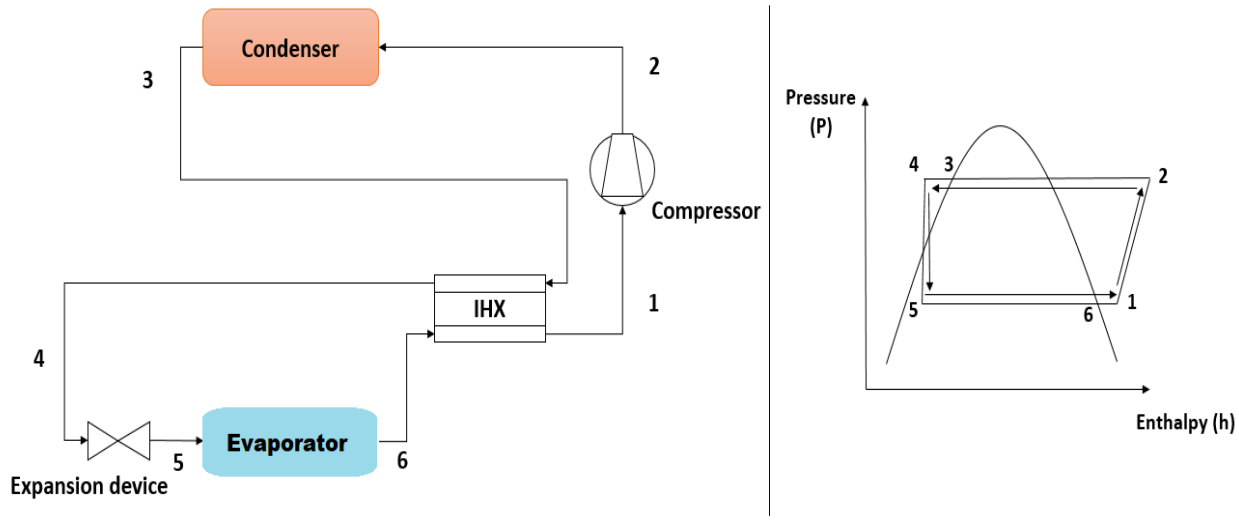

Fig 1. Vapor compression refrigeration cycle with internal heat exchanger (IHX)

An internal heat exchanger (IHX) is incorporated to facilitate heat transfer between the refrigerant leaving the condenser (3-4) and the refrigerant exiting the evaporator (6-1). This setup ensures adequate sub-cooling at the condenser outlet, which reduces the refrigerant's quality at the evaporator inlet while increasing the proportion of latent heat. Additionally, the IHX raises the refrigerant temperature at the evaporator outlet, a phenomenon known as superheating (Méndez-Méndez et al., 2022). These effects are illustrated in the pressure-enthalpy diagram shown in Figure (1).

Table 2. input data to the computational model

Variable	Description	value
Te	Evaporating temperature range	-5°C to 15°C
Tc	Condensation temperature range	25°C to 40°C
N	Compressor rotation speed	2900 rpm
X	IHX thermal effectiveness	80%

We applied the first law of thermodynamics to the system to evaluate its thermodynamic performance. The following assumptions are considered:

- All components are assumed to be under the steady-state process;
- No pressure drops across heat exchangers and heat losses in the compressor are considered;
- The isentropic efficiency of the compressor is associated with the compression ratio;
- The refrigerant’s throttling process is isenthalpic and Kinetic and potential energy changes and exergy losses are neglected.

Based on the assumptions above, the equations for the main components can be derived using the principles of mass, momentum, and energy conservation. The theoretical mass flow rate is expressed as:

$$\dot{m} = VG * \rho suc \left(\frac{N}{60}\right) \quad (1)$$

Here, $V_G = 681.10^{-6}\ m^3$ represents the compressor displacement, ρ_{suc} is the density at the compressor's suction, and N is the rotation number. The system refrigeration capacity is expressed as:

$$Qe = \dot{m}\,(h1 - h5) \quad (2)$$

Where h is the enthalpy. The energy balance in the internal heat exchanger and its thermal effectiveness is expressed as:

$$\dot{m}\,(h1 - h6) = \dot{m}\,(h3 - h4) \quad (3)$$

$$X = (T1 - T6)/\,(T3 - T6) \quad (4)$$

The compressor consumption of power is expressed as:

$$W = \dot{m}\,(h2 - h1) \quad (5)$$

The heat transfer rate in the condenser is given by:

$$Qc = \dot{m}\,(h3 - h2) \quad (6)$$

The coefficient of performance is determined by:

$$COP = Qe/W \quad (7)$$

2.2 The ejection refrigeration system

Figure (2) illustrates the system's schematic layout and the pressure-enthalpy diagram for the associated processes, with the ejector serving as the compression device in this cycle.

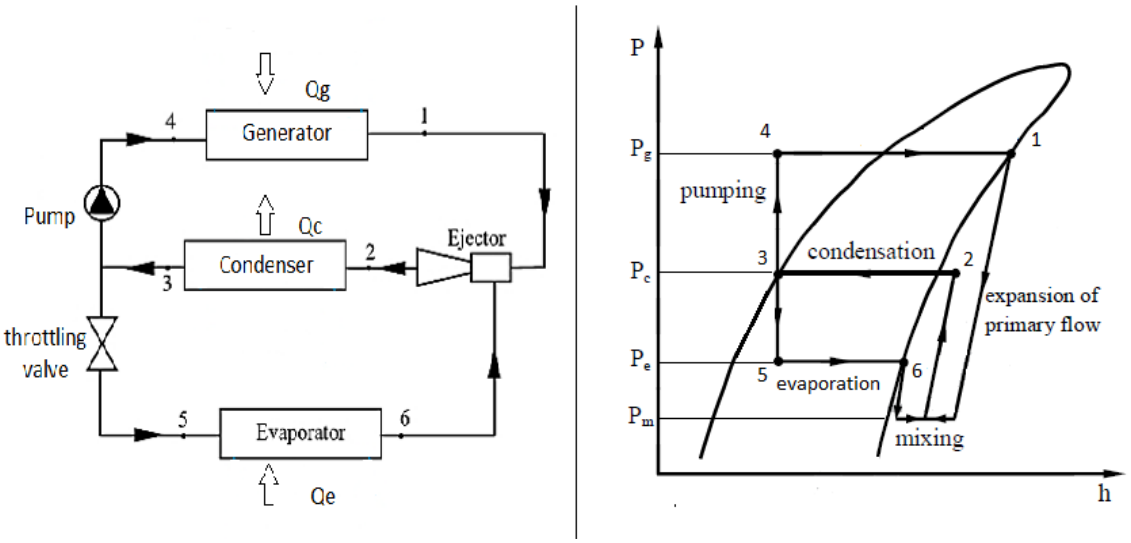

Fig 2. Ejection refrigeration cycle (Saleh, et al, 2016)

Where the high-pressure vapor from the generator (Pg), known as primary flow, expands and accelerates through the ejector nozzle. Then it fans out at a supersonic speed to create a very low pressure (P7p). Consequently, the secondary flow from the evaporator, at pressure (Pe), is drawn into the suction chamber and merges with the primary flow, causing its velocity to increase. Because of the velocity difference, these two flows begin to mix gradually in the mixing chamber, leading the primary flow to be decelerated whilst the secondary flow continues accelerating until they are completely mixed. A normal compression shock occurs at the end of the constant area, leading to a compression effect and a rapid decrease in velocity from supersonic to subsonic. Additional pressure recovery and velocity reduction take place in the diffuser, with the flow eventually exiting into the condenser.

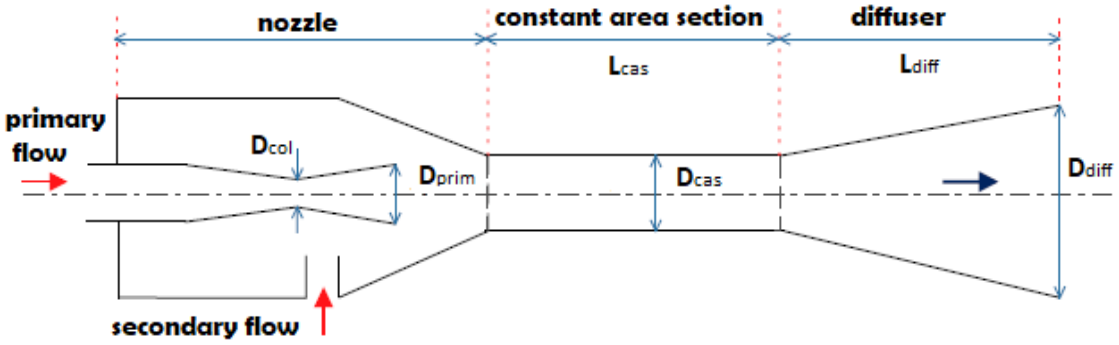

Fig 3. Schematic view of a constant pressure-mixing ejector

Table 3. ejector geometry and polytropic efficiencies (Bencharif et al., 2020)

Geometric parameters	**Value (mm)**
D_{col}	14.42
D_{prim}	22.47
D_{cas}	28.47
D_{diff}	38.10
Polytropic efficiencies	**Value**
Primary nozzle (η_p)	0.96
Secondary flow (η_s)	0.96
Mixing section (η_{mix})	0.90
Diffuser (η_d)	0.85

The thermodynamic model of the ejector is based on the assumption of constant pressure. It solves the mass, momentum, and energy conservation equations, with the following assumptions taken into account:

- The flow within the ejector is steady, one-dimensional, and adiabatic.;
- Fluid properties are uniform at each cross-section and are determined using a real gas model;
- A normal shock occurs before the inlet of the diffuser;
- Losses during the acceleration and compression processes are accounted for using isentropic efficiencies;
- The kinetic energy at the primary nozzle inlet, suction chamber, and diffuser exit is considered negligible;
- The change in potential energy within the ejector is neglected.

The ejector entrainment ratio "μ" is defined as the ratio of the secondary mass flow to the primary mass

flow, expressed as:

$$\mu = \dot{m}s/\dot{m}p \quad (8)$$

The compression ratio P_{cr} is defined as the ratio of the static pressure at the diffuser exit, P_c, to the static pressure of the secondary flow, P_e,

$$Pcr = Pc/Pe \quad (9)$$

2.2.1 Primary inlet and secondary inlet

The primary and secondary flow rates are determined through an iterative process, assuming maximum flux at the throat. This method was employed by (Ameur, et al, 2016). The detailed calculation procedure for these processes is outlined in the following equations:

$$hth = \eta p\,(hth,is - hp) + hp \quad (10)$$

$$hth,is = f\,(Sp\,, Pth) \quad (11)$$

$$Vth = \sqrt{2(hp - hth)} \quad (12)$$

$$\rho th = f\,(Pth\,, hth) \quad (13)$$

$$\dot{m}p = Vth\,\rho th \quad (14)$$

Where "P_{th}" is estimated at the throat while "$h_{th,is}$" and "ρ_{th}" were calculated from COOLPROP.
Same procedure was followed for "Vs" and "ρs" to calculate the secondary flow $\dot{m}_s$, corresponding to sonic conditions:

$$\dot{m}s = Vs\,\rho s \quad (15)$$

2.2.2 Mixing

The mixing of the primary and secondary flows is assumed to take place before the constant area section, the first interaction of both flows leads to the slowing process of the supersonic stream and the Mach number is equal to unity (Ma ≈1):

$$Vmix = (\eta mix\,(Vm + \mu.Vs))/(1 + \mu) \quad (16)$$

2.2.3 Normal shock

At the end of the constant-area section, the pressure of the mixed flow rises, while its velocity decreases to subsonic speeds. Due to the small area, the specific volume of the flow also decreases.

2.2.4 Diffuser

In the diffuser, the kinetic energy of the flow is converted into static pressure, resulting in an increase in pressure and a decrease in velocity. The outlet pressure and temperature of the ejector are determined by the conditions at the end of the constant-area section.
The refrigeration capacity of the system is given by,

$$Qe = \dot{m}s\,(h6 - h5) \quad (17)$$

The rate of heat transfer in the generator is expressed as,

$$\mathrm{Qg} = \dot{m}\mathrm{p}\,(\mathrm{h1} - \mathrm{h4}) \tag{18}$$

The power of the pump is given by:

$$Wp = \dot{m}p\,(h4 - h3) \tag{19}$$

The heat transfer rate in the condenser can be calculated by:

$$\mathrm{Qc} = (\dot{m}\mathrm{s} + \dot{m}\,\mathrm{p})\,(\mathrm{h3} - \mathrm{h2}) \tag{20}$$

The coefficient of performance is determined by:

$$\mathrm{COP} = \mathrm{Qe}/(\mathrm{Qg} + \mathrm{Wp}) \tag{21}$$

When substituting equations (8), (9), and (10) into (12) we get:

$$\mathrm{COP} = \mu\,(\mathrm{h6} - \mathrm{h5})/(\mathrm{h1} - \mathrm{h3}) \tag{22}$$

3. RESULTS AND DISCUSSION

A MATLAB-based computational program was created to model the thermodynamic behavior of both traditional vapor compression refrigeration systems and ejection refrigeration systems. Fluid properties were sourced through integration with COOLPROP. The accuracy of both models was assessed by comparing their outcomes with the experimental findings of (Mota-Babiloni et al., 2014) and (Bencharif et al., 2020).

Table 4. comparison results between the present vapor compression system thermodynamic model and experimental data from Mota-Babiloni et al. (2014) in terms of coefficient of performance.

Te (K)	**Tc (K)**	**Present study COP**	**Mota-Babiloni et al. (2024) COP**	**Deviation %**
260	310	2.47	2.52	-1.9%
260	320	1.93	2.31	-16.4%
270	310	3.72	3.45	7.8%
270	320	2.64	2.75	-4%
280	310	4.71	4.2	12.1%
280	320	3.90	3.66	6.5%

Table 5. comparison results between the present thermodynamic model and experimental data from Bencharif et al. (2020) in terms of entrainment ratio.

Pg (kpa)	**Tg (K)**	**Present study Entrainment ratio "μ"**	**Bencharif et al. (2020) Entrainment ratio**	**Deviation %**
488.956	357.1	0.2373	0.2678	-11.38%
513.681	357.05	0.2150	0.2569	-16.3%
541.914	357.07	0.2105	0.2258	-6.77%
568.611	357.05	0.2090	0.2242	-6.78%
593.139	357.03	0.1990	0.2048	-2.83%
620.004	357.02	0.1877	0.1869	0.42%

The thermodynamic model demonstrated high accuracy in predicting system behavior, as evidenced by its close agreement with experimental data obtained under varying conditions. The model's data points exhibited deviations of no more than ±16% from the experimental results for both the vapor compression and ejector refrigeration systems. These small deviations align with those found in similar models reported in the literature (Bencharif et al., 2020; Croquer et al., 2017). The model's accuracy can be mainly attributed to the accurate thermophysical property calculations provided by CoolProp, which uses advanced equations of state and empirical correlations. It combines a series of non-linear equations with thermophysical property functions, operating under conditions identical to those in the experimental study. Furthermore, the experimental setup was carefully calibrated to reduce external inefficiencies, ensuring precise data. These controlled conditions further minimized potential discrepancies, leading to a strong correlation between the model's predictions and the experimental results used to validate it.

3.1 Performance of the simple vapor compression system

The cooling effect, as depicted in Figure (4) for R134a and the seven other examined refrigerants across varying condensation temperatures **(a)**, reveals a consistent trend. This analysis makes it clear that the cooling capacity (Qe) is inversely proportional to the condensation temperature (Tc) for all investigated refrigerants. Conversely, when exploring different evaporation temperatures **(b)**, it is observed that the cooling capacity (Qe) shows an upward trend with increasing evaporation temperatures (Te). This phenomenon can be attributed to variations in the latent heat value of the refrigerant.

The findings unequivocally indicate that R1270, R717, and R290 surpass R134a in terms of refrigerating effect by 40.6%, 30.07%, and 27.08%, respectively. Therefore very low mass of refrigerant will be required for the same capacity and compressor size. Additionally, it is demonstrated that the (Qe) of R1234yf is nearly identical to that of R134a, making it a promising potential drop-in refrigerant.

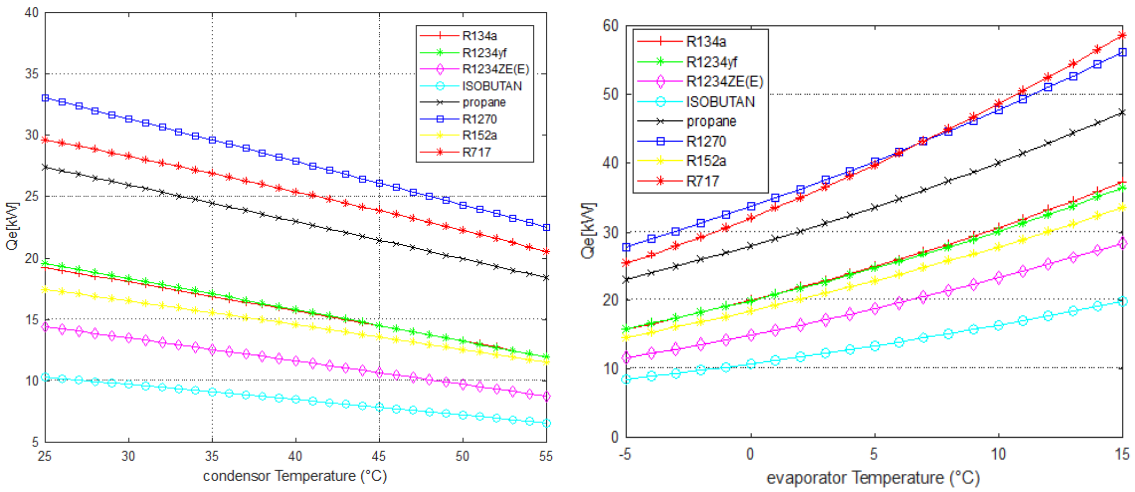

(a) (b)

Fig 4. Variation of (Qe) with the condensation and the evaporation temperatures

As expected, Figure (5) illustrates how the compressor energy input varies with the condensation temperature (Tc) of the examined refrigerants with the evaporation temperature (Te) of -5°C. Notably, it highlights a higher compression energy input for R1270, R717, and R290 in comparison to R134a and other refrigerants that can go up to 10kW when the condensation temperatures reach 45°C. This discrepancy can be attributed to the fact that these refrigerants equally demonstrated a significantly high refrigerating capacity, essentially compensating for their elevated compressor work input.

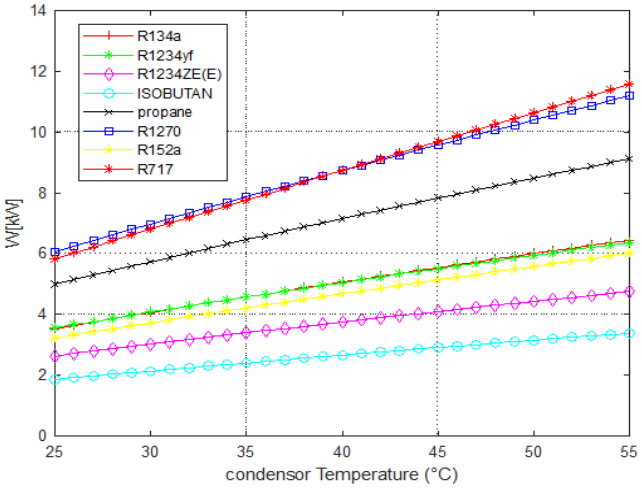

Fig 5. Variation of the compression work with the condensation temperature at Te=-5°C

The Coefficient of Performance (COP) plays a pivotal role in refrigeration, serving as a comprehensive measure of the entire cycle's efficiency and a crucial factor in selecting a new refrigerant. In Figure (6), the COP is depicted at various condenser temperatures (Fig. (a)) and evaporator temperatures (Fig. 6(b)). It is observed that with increasing condensation temperatures (Tc), the Coefficient of Performance (COP) exhibits a declining trend, while there is an upward trend with increasing evaporation temperatures (Te). Both graphs reveals that R717 exhibits the lowest (COP), while R600a (Isobutane) and R290 depicted the highest values among all the investigated refrigerants. When compared to R134a, taking Te=5°C and Tc=40°C, they respectively depicted an improvement of 2.47% and 2.12%. The graphs for most other refrigerants closely resemble that of R134a.

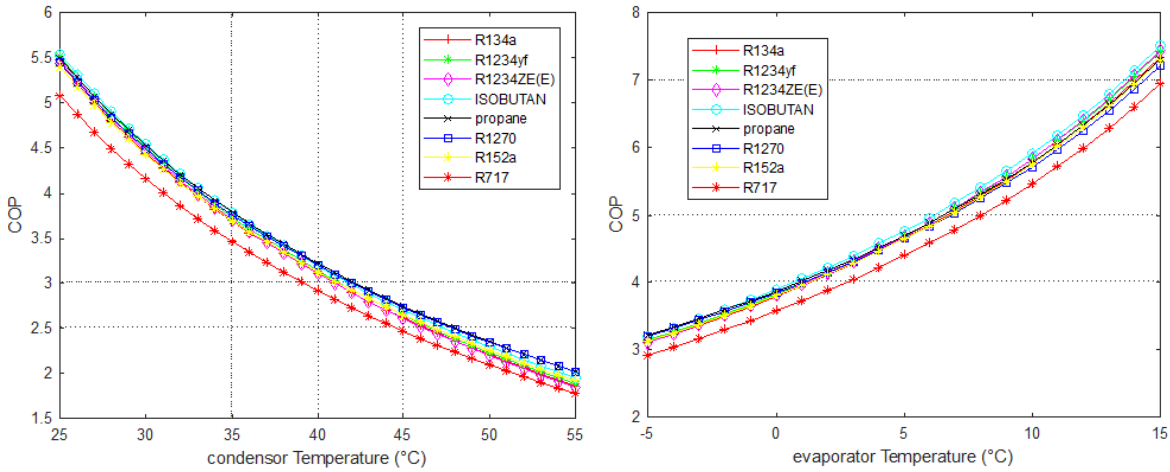

(a) (b)

Fig 6. Variation of (COP) with the condensation and the evaporation temperatures

3.2 Performance of the ejection refrigeration system

The influence of (Tc) and (Te) on generator heat load is illustrated in figure (7) under the selected working conditions for every studied refrigerant. R1270 and R290 (propane exhibited the nearest values to those of the R134a. while R717 and R152a presented the lowest values down to 20 kW, which in terms of energy consumption can reduce the overall energy consumption of the system.

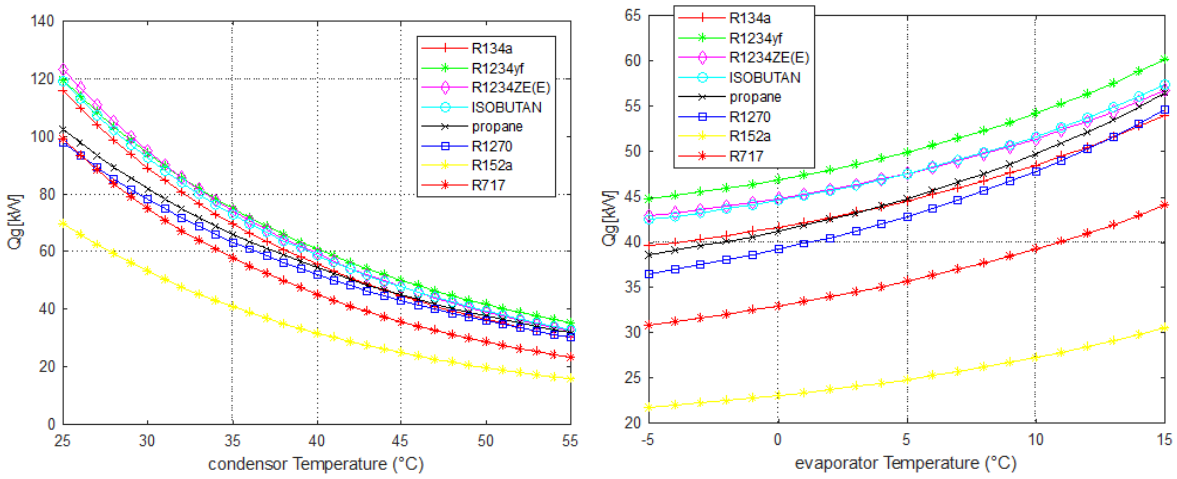

(a) (b)

Fig 7. Variation of (Qg) with the condensation and the evaporation temperatures

The entrainment ratio serves as a metric for assessing ejector performance and efficiency. As depicted in figure (8), the entrainment ratio "μ" for all examined refrigerants demonstrates variations concerning different generator temperatures (Fig. 8(a)) and diverse evaporator temperatures (Fig. 8(b)).

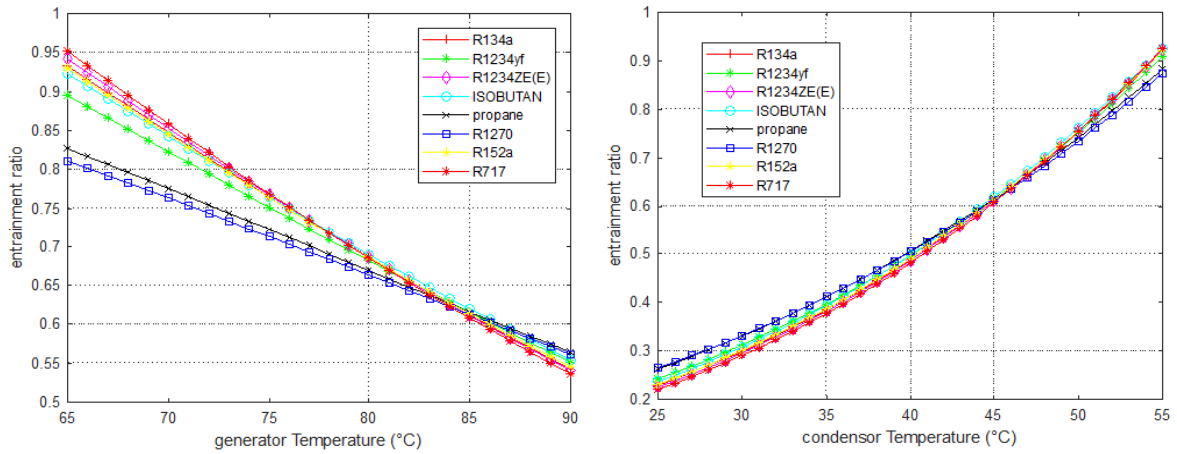

(a) (b)

Fig 8. Variation of the entrainment ratio with the generator and the evaporator temperatures

It is important to note that the entrainment ratio decreases as the generator temperature (Tg) increases, while it increases with higher condenser temperatures (Tc). Both graphs show that the entrainment ratio for R1270, R290, and R1234yf generally falls within the typical range of 0.25 to 0.66 when the generator temperature (Tg) exceeds 85°C and the condenser temperature (Tc) is below 40°C. This indicates the optimal parameter range for these refrigerants.

The coefficient of performance variation with the condenser temperature (a) and the generator temperature (b) in figure (9). It is observed that with increasing condensation temperatures (Tc), the Coefficient of Performance (COP) exhibits a declining trend, while there is an upward trend with the increasing of the generator temperatures (Tg). Both graphs reveals that R1234yf exhibits the lowest (COP) among all the investigated refrigerant. While R152a and R717 depicted the highest values When compared to R134a, taking Tc=45°C and Tg=90°C, they respectively depicted an improvement of 52% and 21.8%. The graphs for most other refrigerants closely align with that of R134a.

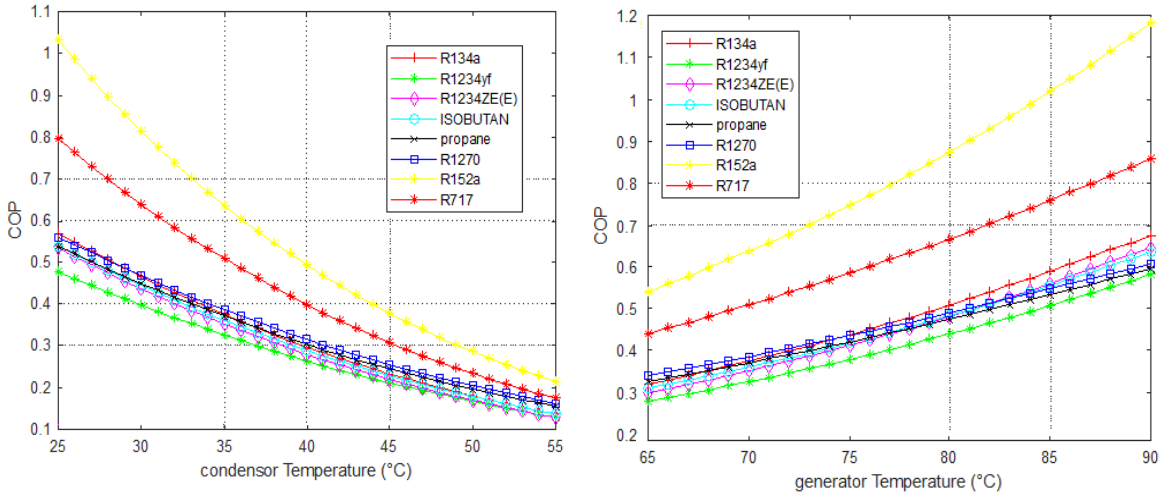

(a) (b)

Fig 9. Variation of the coefficient of performance with the condenser and the generator temperatures

4. CONCLUSION

This study aims to examine the influence of operational factors, such as evaporation temperature, condensation temperature, and generator temperature, on the performance of both a basic vapor compression refrigeration system with an internal heat exchanger and an ejector refrigeration system. The analysis uses energetic methods based on the first and second laws of thermodynamics. Additionally, a comparative assessment between the two systems was conducted to evaluate their performance and determine the most appropriate refrigerant for each configuration. The key findings of this study can be summarized as follows:

- The findings from the vapor compression refrigeration system reveal that, although R1270 and R290 can generate a higher refrigeration load (Qe) compared to R134a, they result in increased energy consumption by the compressor. Conversely, R1234yf exhibits nearly identical values for both (Qe) and compressor work (*W*) when compared to R134a, making it a suitable substitute in a basic vapor compression system. Moreover, in positive temperature conditions, R600a (Isobutane), R290, and R1234yf demonstrate even higher coefficients of performance, namely 2.47%, 2.12%, and 1.66%, respectively, compared to R134a. This substantiates that these refrigerants represent superior alternatives for replacing R134a in traditional compression systems.
- After assessing the ejector entrainment ratio and the coefficient of performance (COP) for ejection refrigeration systems, it has been determined that R152a, R290, and R1270 stand out as the most suitable refrigerants for such installations. Operating with these refrigerants requires a lower generator heat load. While R717 is also a viable option, it is primarily utilized in industrial applications due to certain limitations related to its flammability and toxicity.

These study's findings provide valuable insights for the selection of refrigerants based on specific system requirements, efficiency considerations, and safety constraints. It also highlights the importance of exploring the integration of hybrid systems that combine the strengths of different technologies, aiming for improved overall efficiency and reduced environmental impact. It is also crucial to address the aspect of incorporating non-ideal effects and exploring a broader range of operating conditions to enhance the applicability of our model in future studies.

ACKNOWLEDGEMENTS

The authors would like to thank the LGCC of the University of Constantine "1" for providing the necessary research facilities and space to conduct this research study. We are also grateful for valuable comments and suggestions from reviewers that help to improve our paper quality.

NOMENCLATURE

		Subscripts	
h	specific enthalpy [J.kg^{-1}]	c	condenser
Q	heat load [kW]	e	evaporator
ṁ	mass flow rate [kg.s^{-1}]	g	generator
P	pressure [kPa]	is	isentropic
T	temperature [°C]	p	primary
V_G	compressor displacement [m^3]	s	secondary
W	compressor power consumption [kW]	suc	suction
Wp	power of the pump [kW]	th	throat
X	thermal effectiveness [-]	*Abbreviations*	
Greek symbols		COP	coefficient of performance
ρ	density [kg.m^{-3}]	GWP	global warming potential
μ	entrainment ratio [-]	HFC	hydrofluorocarbons
η	efficiency [-]	IHX	internal heat exchanger
		NBP	normal boiling point
		ODP	ozone depletion potential

REFERENCES

Ameur, K., Aidoun, Z., & Ouzzane, M. (2016). Modeling and numerical approach for the design and operation of two-phase ejectors. Applied Thermal Engineering, 109, 809–818. https://doi.org/10.1016/j.applthermaleng.2014.11.022

Ansari, N. A., Yadav, B., & Kumar, J. (2013). Theoretical Exergy Analysis of HFO-1234yf and HFO-1234ze as an Alternative Replacement of HFC-134a in Simple Vapour Compression Refrigeration System. International Journal of Scientific & Engineering Research, 4(8). http://www.ijser.org

Atmaca, A. U., Erek, A., & Ekren, O. (2017). Investigation of new generation refrigerants under two different ejector mixing theories. Energy Procedia, 136, 394–401. https://doi.org/10.1016/j.egypro.2017.10.271

Bansal, P., & Shen, B. (2015). Analysis of environmentally friendly refrigerant options for window air conditioners. Science and Technology for the Built Environment, 21(5), 483–490. https://doi.org/10.1080/23744731.2015.1016364

Bell, I. H., Wronski, J., Quoilin, S., & Lemort, V. (2014). Pure and pseudo-pure fluid thermophysical property evaluation and the open-source thermophysical property library coolprop. Industrial and Engineering Chemistry Research, 53(6), 2498–2508. https://doi.org/10.1021/ie4033999

Bencharif, M., Nesreddine, H., Perez, S. C., Poncet, S., & Zid, S. (2020). The benefit of droplet injection on the performance of an ejector refrigeration cycle working R245fa. International Journal of Refrigeration, 113, 276–287. https://doi.org/10.1016/j.ijrefrig.2020.01.020

Bobbo, S., Nicola, G. di, Zilio, C., Brown, J. S., & Fedele, L. (2018). Low GWP halocarbon refrigerants: A review of thermophysical properties. In International Journal of Refrigeration (Vol. 90, pp. 181–201). Elsevier Ltd. https://doi.org/10.1016/j.ijrefrig.2018.03.027

Colombo, L. P. M., Lucchini, A., & Molinaroli, L. (2020). Experimental analysis of the use of R1234yf and R1234ze (E) as drop-in alternatives of R134a in a water-to-water heat pump. International Journal of Refrigeration, 115, 18–27. https://doi.org/10.1016/j.ijrefrig.2020.03.004

Croquer, S., Poncet, S., & Aidoun, Z. (2017). Thermodynamic modelling of supersonic gas ejector with droplets. Entropy, 19(11). https://doi.org/10.3390/e19110579

dePaula, C. H., Duarte, W. M., Rocha, T. T. M., de Oliveira, R. N., Mendes, R. de P., & Maia, A. A. T. (2020). Thermo-economic and environmental analysis of a small capacity vapor compression refrigeration system using R290, R1234yf, and R600a. International Journal of Refrigeration, 118, 250–260. https://doi.org/10.1016/j.ijrefrig.2020.07.003

Galindo, J., Dolz, V., García-Cuevas, L. M., & Ponce-Mora, A. (2020). Numerical evaluation of a solar-assisted jet-ejector refrigeration system: Screening of environmentally friendly refrigerants. Energy Conversion and Management, 210. https://doi.org/10.1016/j.enconman.2020.112681

Méndez-Méndez, D.; Pérez-García, V.; Belman-Flores, J.M.; Riesco-Ávila, J.M.; Barroso-Maldonado, J.M. Internal Heat Exchanger Influence in Operational Cost and Environmental Impact of an Experimental Installation Using Low GWP Refrigerant for HVAC Conditions. Sustainability 2022, 14, 6008. https://doi.org/10.3390/su14106008

Mota-Babiloni, A., Navarro-Esbrí, J., Barragán, Á., Molés, F., & Peris, B. (2014). Drop-in energy performance evaluation of R1234yf and R1234ze(E) in a vapor compression system as R134a replacements. Applied Thermal Engineering, 71(1), 259–265. https://doi.org/10.1016/j.applthermaleng.2014.06.056

"Official Journal of the European Union," Directive 2006/40/EC of the European Parliament and of the Council, 14.6.2006.

Ozsipahi, M., Kose, H. A., Kerpicci, H., & Gunes, H. (2022). Experimental study of R290/R600a mixtures in vapor compression refrigeration system. International Journal of Refrigeration, 133, 247–258. https://doi.org/10.1016/j.ijrefrig.2021.10.004

Saleh, B. (2016). Performance analysis and working fluid selection for ejector refrigeration cycle. Applied Thermal Engineering, 107, 114–124. https://doi.org/10.1016/j.applthermaleng.2016.06.147

Sánchez, D., Andreu-Nácher, A., Calleja-Anta, D., Llopis, R., & Cabello, R. (2022). Energy impact evaluation of different low-GWP alternatives to replace R134a in a beverage cooler. Experimental analysis and optimization for the pure refrigerants R152a, R1234yf, R290, R1270, R600a and R744. Energy Conversion and Management, 256. https://doi.org/10.1016/j.enconman.2022.115388

Sánchez, D., Cabello, R., Llopis, R., Arauzo, I., Catalán-Gil, J., & Torrella, E. (2017). Évaluation de la performance énergétique du R1234yf, du R1234ze(E), du R600a, du R290 et du R152a comme alternatives à faible GWP au R134a. International Journal of Refrigeration, 74,267–280. https://doi.org/10.1016/j.ijrefrig.2016.09.020

Tashtoush, B., & Bani Younes, M. (2019). Comparative Thermodynamic Study of Refrigerants to Select the Best Environment-Friendly Refrigerant for Use in a Solar Ejector Cooling System. Arabian Journal for Science and Engineering, 44(2), 1165–1184. https://doi.org/10.1007/s13369-018-3427-4

Zheng, H., Tian, G., Zhao, Y., Jin, C., Ju, F., & Wang, C. (2022). Experimental study of R290 replacement R134a in cold storage air conditioning system. Case Studies in Thermal Engineering, 36. https://doi.org/10.1016/j.csite.2022.10220

Zyczkowski, P., Borowski, M., Łuczak, R., Kuczera, Z., & Ptaszyński, B. (2020). Functional equations for calculating the properties of low-GWP R1234ze (E) refrigerant. *Energies*, *13*(12). https://doi.org/10.3390/en13123052